Inorganic Chemistry

Article

Enhanced Photocatalysis of Rhenium(I) Complex by Light-Harvesting Periodic Mesoporous Organosilica

Hiroyuki Takeda,[†,§] Masataka Ohashi,[†,§] Takao Tani,[†,§] Osamu Ishitani,*[‡,§] and Shinji Inagaki*[†,§]

[†]*Toyota Central R&D Laboratories, Inc., Nagakute, Aichi 480-1192, Japan,* [‡]*Department of Chemistry, Graduate School of Science and Engineering, Tokyo Institute of Technology, 2-12-1-E1-9 O-okayama, Meguro-ku, Tokyo 152-8551, Japan, and* [§]*Core Research for Evolutional Science and Technology* (*CREST*), *Japan Science and Technology Agency* (*JST*), *Kawaguchi, Saitama 332-0012, Japan*

This paper describes a new conceptual design for enhancement of photocatalytic CO_2 reduction of a rhenium(I) complex by light harvesting of periodic mesoporous organosilica (PMO). Mesoporous biphenyl-silica (Bp-PMO) anchoring *fac*-[Re[I](bpy)(CO)$_3$(PPh$_3$)]$^+$(OTf)$^-$ (bpy =2,2′-bipyridine; OTf = CF$_3$SO$_3$) in the mesochannels was synthesized by co-condensation of two organosilane precursors, 4,4′-bis(triethoxysilyl)biphenyl and 4-[4-{3-(trimethoxysilyl)propylsulfanyl}butyl]-4′-methyl-2,2′-bipyridine in the presence of a template surfactant, followed by coordination of a rhenium precursor, [Re[I](CO)$_5$(PPh$_3$)]$^+$(OTf)$^-$ to the bipyridine ligand in the mesochannels. The 280 nm light was effectively absorbed by the biphenyl groups in Bp-PMO, and the excited energy was funneled into the Re complex by resonance energy transfer, which enhanced photocatalytic CO evolution from CO_2 by a factor of 4.4 compared with direct excitation of the Re complex. Bp-PMO had an additional merit to protect the Re complex against a decomposition by UV irradiation. These results demonstrate the potential of PMOs as a light-harvesting antenna for designing various photoreaction systems, mimicking the natural photosynthesis.

Introduction

Solar energy conversion systems that involve water splitting[1] and CO_2 reduction[2] photocatalysts are attracting much attention as an alternative to energy production from fossil fuels.[3] The development of CO_2 reduction photocatalysts is particularly important with respect to recycling of exhausted CO_2 into useful fuels and organic compounds.[4a] Natural photosynthesis shows the efficient photocatalysis of CO_2 reduction to form carbohydrates. One of the key components of natural photosynthesis is a light-harvesting antenna, typically observed as wheel-like arrays of chlorophylls in LH1 and LH2 of purple photosynthetic bacteria, which absorbs sunlight effectively and funnel the captured energy to a reaction center by resonance energy transfer (RET) with

a quantum efficiency of almost unity.[4] For construction of artificial photosynthesis systems, the three-dimensional organization of molecular parts, that is, light absorbers and multielectron catalysts, at appropriate positions is of particular importance, because the RET efficiency is strongly dependent on the distance between the energy donor and acceptor molecules and their orientation.[5]

A range of supramolecular antenna systems, such as dendrimers,[5b] porphyrin arrays,[5b] organogels,[6] dye-loaded zeolites,[7] and photoactive polymers,[5a] with controlled three-dimensional architectures have been reported and exhibit strong light-absorption and efficient funneling of captured energy into a small amount of acceptors by RET. However, it has not been reported to construct supramolecular photocatalyst systems for CO_2 reduction with an efficient light-harvesting antenna like in the natural photosynthesis. The limited application of the conventional supramolecular antenna materials to a RET type photocatalysis system is mainly

*To whom correspondence should be addressed. E-mail: ishitani@chem.titech.ac.jp (O.I.), inagaki@mosk.tytlabs.co.jp (S.I.).
(1) (a) Maeda, K.; Domen, K. *J. Phys. Chem. C* **2007**, *111*, 7851–7861. (b) Wang, X.; Maeda, K.; Thomas, A.; Takanabe, K.; Xin, G.; Carlsson, J. M.; Domen, K.; Antonietti, M. *Nat. Mater.* **2009**, *8*, 76–80. (c) Kudo, A.; Miseki, Y. *Chem. Soc. Rev.* **2009**, *38*, 253–278. (d) Dempsey, J. L.; Esswein, A. J.; Manke, D. R.; Rosenthal, J.; Soper, J. D.; Nocera, D. G. *Inorg. Chem.* **2005**, *44*, 6879–6892. (e) Du, P.; Schneider, J.; Luo, G.; Brennessel, W. W.; Eisenberg, R. *Inorg. Chem.* **2009**, *48*, 4952–4962.
(2) (a) Arakawa, H.; et al. *Chem. Rev.* **2001**, *101*, 953–996. (b) Fujita, E. *Coord. Chem. Rev.* **1999**, *185–186*, 373–384. (c) Takeda, H.; Ishitani, O. *Coord. Chem. Rev.* **2010**, *254*, 346–354.
(3) Lewis, N. S.; Nocera, D. G. *Proc. Natl. Acad. Sci. U.S.A.* **2006**, *103*, 15729–15735.

(4) (a) Pullerits, T.; Sundström, V. *Acc. Chem. Res.* **1996**, *29*, 381–389. (b) Pascal, A. A.; Liu, Z.; Broess, K.; van Oort, B.; van Amerongen, H.; Wang, C.; Horton, P.; Robert, B.; Chang, W.; Ruban, A. *Nature* **2005**, *436*, 134–137.
(5) (a) Alstrum-Acevedo, J. H.; Brennaman, M. K.; Meyer, T. J. *Inorg. Chem.* **2005**, *44*, 6802–6827. (b) Balzani, V.; Credi, A.; Venturi, M. *ChemSusChem* **2008**, *1*, 26–58.
(6) Ajayaghosh, A.; Praveen, V. K. *Acc. Chem. Res.* **2007**, *40*, 644–656.
(7) Calzaferri, G.; Lutkouskaya, K. *Photochem. Photobiol. Sci.* **2008**, *7*, 879–910.

attributed to difficulty in the organization of chromophores and binding of reaction sites at appropriate positions in the antenna and/or limited internal void space that hinders efficient mass transfer for catalytic reactions.

Periodic mesoporous organosilicas (PMOs)[8] are a new class of functional materials with well-defined mesopores and organic−inorganic hybrid frameworks in a supramolecular architecture of organic moieties covalently fixed within a siloxane network. They have been revealed to show unique fluorescence,[9] hole-transportation,[10] and electron donation properties.[11] Recently, the organosilica framework was also found to exhibit unique light-harvesting antenna properties; funneling of light energy absorbed by approximately 125 chromophores of the framework into a single dye molecule doped in the mesochannels by RET, with almost 100% quantum efficiency.[12] The well-defined mesopores of PMOs, whose pore can be controlled in the range of 1.5−30 nm in diameter, are also advantageous for the construction of heterogeneous photocatalysis systems, because (i) photoactive species can be placed precisely in the pore space[13] into which light energy is funneled, and (ii) sufficient internal void spaces for efficient mass transfer can be retained, even after the placement of photocatalysts, because of larger pore sizes[14] compared with those of layered compounds,[15] and zeolites.[16] Furthermore, the high surface areas of mesoporous structures can increase reaction sites and thus enhance photocatalytic activity. Therefore, PMOs are considered to have a potential as a solid-state supramolecular light-harvesting antenna for enhancement of photocatalysis.

This paper describes a new conceptual design for enhancement of photocatalytic CO_2 reduction of a rhenium(I) complex placed in the mesochannels of PMO by its light-harvesting antenna property. A rhenium (Re) bipyridine complex was chosen as a reaction center because it is well-known two-electron-reduction photocatalysis of CO_2
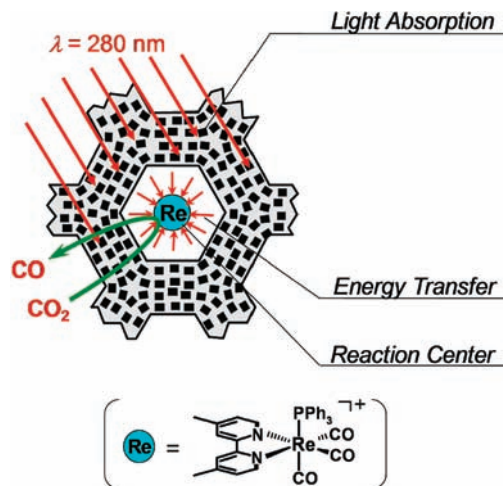

Figure 1. Schematic representation of light-harvesting by PMO and enhancing of photocatalysis of Re complex.

to CO.[2b,c,17] A PMO with biphenyl chromophores in the framework (Bp-PMO)[8f,9c,12a] was used as a light-harvesting antenna because of its well-studied optical properties and good spectral overlap of its emission band with the absorption band of the Re bipyridine complex for efficient RET. An elegant route for covalent immobilization of the Re complex was developed to fix them homogeneously within appropriate distances from Bp (light absorber) in the framework also for efficient RET. The obtained system successfully funneled the light energy absorbed in the framework into the Re complex, placed in the mesochannels and enhanced photocatalytic reduction of CO_2 (Figure 1).

Experimental Section

Chemicals. All reagents and solvents were of highest commercial quality and used without further purification. The organosilane precursors, 1,4-bis(triethoxysilyl)biphenyl (BTEBP, $(C_2H_5O)_3Si−C_6H_4C_6H_4−Si(OC_2H_5)_3$, MW = 478.73) and 4-[4-{3-(trimethoxysilyl)propylsulfanyl}butyl]-4′-methyl-2,2′-bipyridine[18] (SiBPy, $(CH_3O)_3Si−C_3H_6−S−C_4H_8−C_{11}N_2H_9$, MW = 420.65), were purchased from Nard Institute, Ltd., Japan. The cationic surfactant, octadecyltrimethylammonium chloride (C_{18}TMACl, $C_{18}H_{37}N(CH_3)_3Cl$, MW = 348.05) was purchased from TCI. The Bp-PMO powder was synthesized according to the literature.[8f] fac-[Re(dmb)(CO)$_3$(PPh$_3$)](PF$_6$) (dmb = 4,4′-dimethyl-2,2′-bipyridine) was prepared by a literature method.[19]

Synthesis of BPy-Bp-PMO Powder. A mixture of BTEBP (5.63 g) and SiBPy (3.12 g) was slowly added to a mixture of C_{18}TMACl (6.7 g), 6 M sodium hydroxide (18 mL), and deionized water (240 g). The suspension was sonicated for 20 min, stirred at room temperature (rt) for 18 h, and heated at 95 °C for further 20 h under a static condition. The resultant white precipitate was recovered by filtration, washed with water, and finally vacuumed-dried to yield the as-made BPy-Bp-PMO powder. The surfactant was extracted from the as-made material by refluxing the obtained powder (1 g) in ethanol (200 mL) added with conc. hydrochloric acid (9 g). The extraction treatment was repeated twice. Finally, the surfactant-free

(8) (a) Hoffmann, F.; Cornelius, M.; Morell, J.; Fröba, M. *Angew. Chem., Int. Ed.* **2006**, *45*, 3216–3251. (b) Kapoor, M. P.; Inagaki, S. *Bull. Chem. Soc. Jpn.* **2006**, *79*, 1463–1475. (c) Fujita, S.; Inagaki, S. *Chem. Mater.* **2008**, *20*, 891–908. (d) Inagaki, S.; Guan, S.; Fukushima, Y.; Ohsuna, T.; Terasaki, O. *J. Am. Chem. Soc.* **1999**, *121*, 9611–9614. (e) Inagaki, S.; Guan, S.; Ohsuna, T.; Terasaki, O. *Nature* **2002**, *416*, 306–307. (f) Kapoor, M. P.; Yang, Q.; Inagaki, S. *J. Am. Chem. Soc.* **2002**, *124*, 15176–15177.

(9) (a) Goto, Y.; Mizoshita, N.; Ohtani, O.; Okada, T.; Shimada, T.; Tani, T.; Inagaki, S. *Chem. Mater.* **2008**, *20*, 4495–4498. (b) Mizoshita, N.; Goto, Y.; Tani, T.; Inagaki, S. *Adv. Funct. Mater.* **2008**, *18*, 3699–3705. (c) Tani, T.; Mizoshita, N.; Inagaki, S. *J. Mater. Chem.* **2009**, *19*, 4451–4456. (d) Mizoshita, N.; Goto, Y.; Kapoor, M. P.; Shimada, T.; Tani, T.; Inagaki, S. *Chem.—Eur. J.* **2009**, *15*, 219–226. (e) Mizoshita, N.; Goto, Y.; Tani, T.; Inagaki, S. *Adv. Mater.* **2009**, *21*, 4798–4801.

(10) Mizoshita, N.; Ikai, M.; Tani, T.; Inagaki, S. *J. Am. Chem. Soc.* **2009**, *131*, 14225–14227.

(11) Ohashi, M.; Aoki, M.; Yamanaka, K.; Nakajima, K.; Ohsuna, T.; Tani, T.; Inagaki, S. *Chem.—Eur. J.* **2009**, *15*, 13041–13046.

(12) (a) Inagaki, S.; Ohtani, O.; Goto, Y.; Okamoto, K.; Ikai, M.; Yamanaka, K.; Tani, T.; Okada, T. *Angew. Chem., Int. Ed.* **2009**, *48*, 4042–4046. (b) Ito, S.; Fukuya, S.; Kusumi, T.; Ishibashi, Y.; Miyasaka, H.; Goto, Y.; Ikai, M.; Tani, T.; Inagaki, S. *J. Phys. Chem. C* **2009**, *113*, 11884–11891.

(13) (a) Itoh, T.; Yano, K.; Inada, Y.; Fukushima, Y. *J. Am. Chem. Soc.* **2002**, *124*, 13437–13441. (b) Furukawa, H.; Kuroda, K.; Watanabe, T. *Chem. Commun.* **2001**, 2002–2003.

(14) (a) Lin, W.; Frei, H. *J. Am. Chem. Soc.* **2005**, *127*, 1610–1611. (b) Sung-Suh, H. M.; Kim, D. S.; Lee, C. W.; Park, S.-E. *Appl. Organomet. Chem.* **2000**, *14*, 826–830.

(15) Takagi, S.; Eguchi, M.; Tryk, D. A.; Inoue, H. *Langmuir* **2006**, *22*, 1406–1408.

(16) (a) Borja, M.; Dutta, P. K. *Nature* **1993**, *362*, 43–45. (b) Yoon, K. B. *Chem. Rev.* **1993**, *93*, 321–329. (c) Krueger, J. S.; Mayer, J. E.; Mallouk, T. E. *J. Am. Chem. Soc.* **1988**, *110*, 8232–8234.

(17) (a) Hawecker, J.; Lehn, J.-M.; Ziessel, R. *Helv. Chim. Acta* **1986**, *69*, 1990–2012. (b) Kurz, P.; Probst, B.; Spingler, B.; Alberto, R. *Eur. J. Inorg. Chem.* **2006**, 2966–2974. (c) Takeda, H.; Koike, K.; Inoue, H.; Ishitani, O. *J. Am. Chem. Soc.* **2008**, *130*, 2023–2031.

(18) Nguyen, J. V.; Jones, C. W. *Macromolecules* **2004**, *37*, 1190–1203.

(19) Tsubaki, H.; Sekine, A.; Ohashi, Y.; Koike, K.; Takeda, H.; Ishitani, O. *J. Am. Chem. Soc.* **2005**, *127*, 15544–15555.

BPy-Bp-PMO (3.27 g) was treated with a 0.5 M triethylamine ethanol solution (100 mL) for one night to neutralize the bipyridine ligands which had been protonated during the surfactant extraction process. The elemental analysis of sulfur (S) indicates 0.47 mmol g^{-1} of S in BPy-Bp-PMO, which suggests that the same amount of BPy are attached in Bp-PMO because the S−C bond cleavage does not usually occurr in the synthesis condition.

Synthesis of Re/Bp-PMO Powder. [Re(CO)$_5$(PPh$_3$)]$^+$(OTf)$^-$ (OTf = CF$_3$SO$_3$) was prepared according to the literature.[20] The BPy-Bp-PMO powder (300 mg) was dispersed in a toluene solution of [Re(CO)$_5$(PPh$_3$)]$^+$(OTf)$^-$ (104 mg, 0.141 mmol in 60 mL of toluene), and refluxed for 5 h under an argon atmosphere. After cooling to room temperature the resultant yellow powder was recovered by filtration, repeatedly washed with toluene and acetone, and vacuum dried. The incorporated amount of Re in Re/Bp-PMO was determined by inductively coupled plasma (ICP) analysis of both the PMO powder and the residuals in the filtrate, which showed a good mass balance. The amount of Re in Re/Bp-PMO was 0.29 mmol g^{-1}, indicating that 79 mol % of the bipyridine ligands formed [Re(dmb)-(CO)$_3$(PPh$_3$)]$^+$ complex in Re/Bp-PMO.

General Measurements. The UV−vis diffuse reflectance (DR) spectra were recorded on a JASCO V-670 spectrophotometer with an integrating sphere unit (JASCO ISN-723). The longitudinal axes of the spectrum were converted using the Kubelka−Munk function from reflectance (%R) to K/S unit. The emission spectra were measured by a JASCO FP6500 spectrofluorometer. The PMO powder (1.0 mg) was dispersed in CH$_3$CN (4 mL) and degassed by Ar bubbling prior to the measurement. The nitrogen adsorption/desorption isotherms were measured using a Quantachrome Nova-3000e sorptometer at −196 °C. Prior to the measurements, the samples were outgassed at 60 °C for 4 h. The Brunauer−Emmett−Teller (BET) surface areas were calculated from a linear section of the BET plot ($P/P_0 = 0.05-0.2$). The DFT (Density Functional Theory) pore diameter was calculated using a DFT kernel (N$_2$ at 77 K on silica, cylindrical pore, NLDFT equilibrium model). The transmission electron microscopic (TEM) observation was conducted using a JEOL JEM-2000EX microscope. For observation, the powder sample was dispersed in ethanol after grinding with a mortar and deposited to a supporting grid. The powder X-ray diffraction (XRD) patterns were measured on a Rigaku RINT-TTR diffractometer with Cu Kα radiation (50 kV, 300 mA).

Photocatalytic Reaction. The Re/Bp-PMO powder (10 mg) was dispersed in a 5:1 v/v mixed solution (50 mL) of CH$_3$CN (Aldrich Biotech grade, > 99.93%) and triethanolamine (TEOA, Fluka 99.5%) as a sacrificial reductant. The suspension was introduced in a pyrex vessel covered with a quartz cap equipped with a pit reaching to the liquid surface in the vessel for insertion of an optical fiber. The vessel was connected to a closed gas circulation and evacuation system, and then degassing under vacuum and purging of CO$_2$ (Taiyo Nippon Sanso 99.9%) gas were repeated three times to remove air from the reactor, and finally CO$_2$ was introduced until an inner pressure reached 1 atm. The light was irradiated from an end of a fiber with a 300 W xenon lamp (Asahi spectra, MAX-301) equipped with a mirror module and a band-pass filter (280 or 365 nm, half-width of 10 nm). The irradiated-light intensity was monitored with a Molectron PowerMAX500AD power meter and adjusted to 1.7×10^{-8} einstein/s^{-1} with a ND filter. The reactor was kept at 20 °C in a thermostat bath (As-one CB-15). The suspension was stirred with a magnetic bar, and the upper gas phase was pumped and circulated through the suspension during the photoreaction. A fraction of the gas phase was sampled and analyzed using a Shimadzu GC-8A gas-chromatograph (GC) equipped with a

thermal conductivity detector (TCD) and an active carbon (mesh 60/80, 3 m long) column (Supporting Information, Figure S1). For comparison, the photocatalysis test was carried out also for a 50 mL homogeneous solution containing rhenium(I) complex, *fac*-[Re(dmb)(CO)$_3$(PPh$_3$)](PF$_6$) (0.06 mM) instead of the Re/Bp-PMO suspension.

Quantum Yield of CO Formation. An apparent quantum yield of CO formation was determined using a following equation:

$$\Phi_{CO}{}^{app} = (\text{number of CO formed [mol]})/$$
$$(\text{number of irradiated photon [einstein]})$$

Characterization of Rhenium Complex after Photoreaction. The infrared (IR) spectra of the Re complex after the photoreactions were recorded on a Nicolet AVATAR-360 spectrometer. The Re/Bp-PMO powder (1.5 mg) before and after the photocatalytic reaction was diluted with KBr (300 mg) by mixing and pelleted (200 mg) for IR measurements. The Re complex after homogeneous photoreactions was characterized by IR and electrospray ionization mass spectroscopy (ESI-MS) (using a Micromass Q-TOF mass-spectrometer), after extraction with CH$_2$Cl$_2$/H$_2$O into a CH$_2$Cl$_2$ phase, evaporation of CH$_2$Cl$_2$, and redissolution with CH$_3$CN, to avoid baseline perturbation by TEOA contained in the reaction solution.

^{13}CO$_2$ Tracer Experiment. ^{13}CO$_2$ (ISOTEC, > 99 atom % ^{13}C) instead of CO$_2$ was used for the photocatalysis test. After photoirradiation, a fraction of the gas phase was collected and analyzed by the same method as described above using GC-TCD for determination of a total amount of CO formed. Furthermore, the gas in the reactor was trapped as solid with liquid N$_2$ cooling and vaporized in a sample bag. Then, the gasphase containing CO formed was analyzed using an Agilent 6890−5973 gas chromatograph-mass spectrometer (GC-MS) for determination of a fraction of ^{13}CO in CO formed. After the photocatalytic reaction, the Re/Bp-PMO powder was recovered by filtration and analyzed by IR spectroscopy (Attenuated Total Reflection; ATR).

Results and Discussion

Re/Bp-PMO powder was prepared by two step processes as shown in Figure 2. In the first step, Bp-PMO anchoring bipyridine (BPy) ligands on the walls of the mesochannels with Si−O−Si covalent bonds (BPy-Bp-PMO) was obtained by co-condensation of two-organosilane precursors, BTEBP and SiBPy, in the presence of a C$_{18}$TMACl surfactant template under a basic condition. In this route, BPy can be homogeneously dispersed,[8a,21] especially in the mesochannels because the bipyridine unit and the attached alkyl chain are hydrophobic in nature and tend to enter into a core of the rod like surfactant micelles during the co-condensation process,[8b,22] which can promote homogeneous fixation of the Re complex in the mesochannels. The rhenium bipyridine complex, *fac*-[Re(BPy)(CO)$_3$(PPh$_3$)]$^+$(OTf)$^-$ (BPy = the bipyridine unit anchored on the walls of the mesochannels) was formed by subsequent coordination of [Re(CO)$_5$(PPh$_3$)]$^+$-(OTf)$^-$ to the bipyridine unit in BPy-Bp-PMO by refluxing in a toluene suspension.

The transmission electron microscopy (TEM) (Figure 3a) confirmed the successful formation of an ordered mesoporous

(20) Nitschke, J.; Schmidt, S. P.; Trogler, W. C. *Inorg. Chem.* **1985**, *24*, 1972–1978.

(21) Ariga, K.; Vinu, A.; Hill, J. P.; Mori, T. *Coord. Chem. Rev.* **2007**, *251*, 2562–2591.

(22) (a) Yang, Q.; Kapoor, M. P.; Inagaki, S. *J. Am. Chem. Soc.* **2002**, *124*, 9694–9695. (b) Huh, S.; Wiench, J. W.; Yoo, J.-C.; Pruski, M.; Lin, V. S.-Y. *Chem. Mater.* **2003**, *15*, 4247–4256. (c) Kapoor, M. P.; Yang, Q.; Goto, Y.; Inagaki, S. *Chem. Lett.* **2003**, *32*, 914–915.

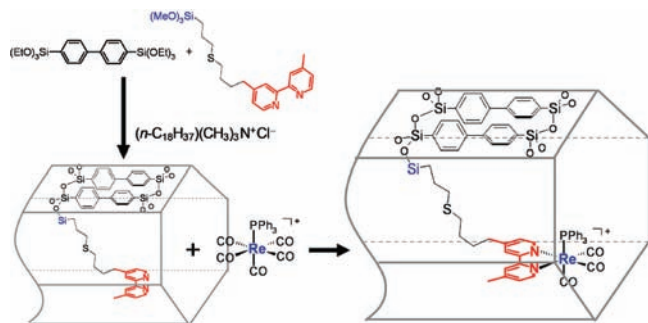**Figure 2.** Schematic representation of two-step synthesis of a rhenium-(I) bipyridine complex ([Re(BPy)(CO)$_3$(PPh$_3$)]$^+$) fixed in biphenyl-bridged periodic mesoporous organosilica (Re/Bp-PMO).
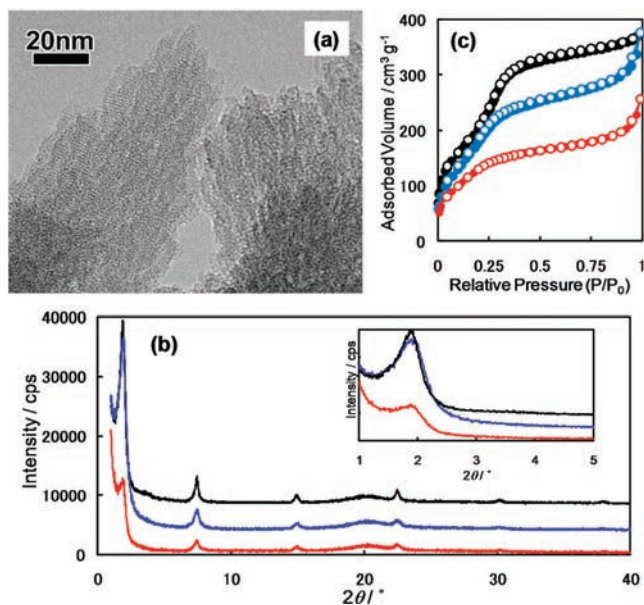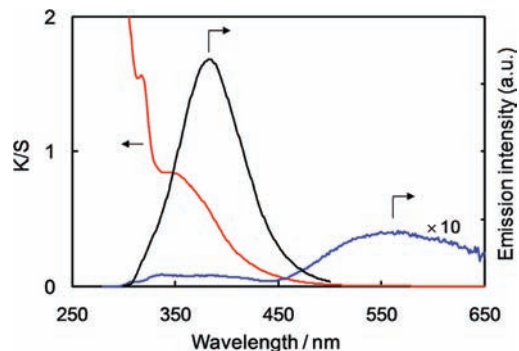

Figure 4. UV−vis diffuse reflectance spectrum of Re/Bp-PMO (red line) and emission spectra of Bp-PMO (black) and Re/Bp-PMO (blue) excited at 260 nm.
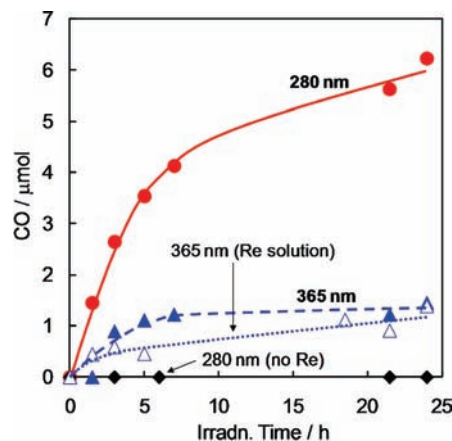

Figure 3. Structural properties of Re/Bp-PMO. (a) TEM image of Re/Bp-PMO, (b) XRD patterns and (c) nitrogen adsorption/desorption isotherms at 77 K: the Bp-PMO (black), BPy-Bp-PMO (blue), and Re/Bp-PMO (red).

Figure 5. CO generation by photocatalysis for CO$_2$ reduction on Re/Bp-PMO (Re: 3 μmol) under photoirradiation at 280 (●) and 365 nm (▲), and in a homogeneous [Re(dmb)(CO)$_3$(PPh$_3$)]$^+$ solution (0.06 mM; Re: 3 μmol) under photoirradiation at 365 nm (△). No CO generation was observed for Bp-PMO without the Re complex under photoirradiation at 280 nm (◆).

structure consisting of one-dimensional uniform channels and periodic arrangement of Bp in the pore walls[8f] of Re/Bp-PMO without any dark spots corresponding to metallic clusters. The XRD patterns (Figure 3b) of Re/Bp-PMO and BPy-Bp-PMO also reflected the existence of ordered mesochannels ($2\theta = 1.9°$) along with lamellar periodicity of the organic bridges in the pore walls ($2\theta = 6-40°$).[8f] The nitrogen adsorption/desorption isotherms revealed that Re/Bp-PMO had large pore-volume (0.21 cm^3 g^{-1}), specific surface area (520 m^{2}g^{-1}) and pore-diameter (2.9 nm), sufficient for mass transfer and catalytic reactions (Figure 3c). The pore-volume of Re/Bp-PMO was smaller than those of Bp-PMO (0.49 cm^3 g^{-1}) and BPy-Bp-PMO (0.33 cm^3 g^{-1}) without any change in *d*-value (4.7 nm), which indicates that the Re complexes were mostly located within the mesochannels, because the decrease in pore-volume agreed well with the volume estimated from the molecular volume ([Re(BPy)(CO)$_3$(PPh$_3$)](OTf), 859.3 Å^3) and the number of the Re complex introduced in Bp-PMO. The elemental analysis showed that the content of the Re complex in Re/Bp-PMO was 0.43 mmol g^{-1}-Bp-PMO, which corresponds to a Re/Bp molar ratio of 0.11 (Bp in Bp-PMO was 3.77 mmol g^{-1}).

The UV−vis diffuse reflectance spectrum of Re/Bp-PMO (Figure 4: red) shows a metal-to-ligand charge transfer (MLCT) absorption band ($\lambda_{max} = 345$ nm) which corresponds to that of *fac*-[Re(dmb)(CO)$_3$(PPh$_3$)]$^+$ (dmb = 4,4′-dimethyl-2,2′-bipyridine) in CH$_3$CN ($\lambda_{max} = 340$ nm).[23] The ν(C≡O) peaks at 2040, 1950, and 1930 cm^{-1} in the Fourier transform infrared (FT-IR) spectrum of Re/Bp-PMO indicate *fac*-Re(CO)$_3$ symmetry, in agreement with those of *fac*-[Re(dmb)(CO)$_3$(PPh$_3$)]$^+$ (2037, 1948, and 1925 cm^{-1} in CH$_3$CN; data not shown).

Figure 4 also displays the emission spectra of Bp-PMO and Re/Bp-PMO excited at 260 nm. Bp-PMO showed strong fluorescence ($\lambda_{max} = 380$ nm, $\Phi = 0.42 \pm 0.02$) because of the biphenyl groups in the framework,[12a] whereas Re/Bp-PMO showed almost no emission from the biphenyl group but exhibited a new emission band at 450−700 nm because of the Re complex. The results suggest that the excitation energy of the biphenyl groups is completely transferred into the Re complex in spite of the low Re/Bp molar ratio. Although the Re complexes also absorb the excitation light (260 nm), their contribution is estimated to be quite low (~5%), with consideration of the molar extinction coefficients (ε) in CH$_3$CN ($\varepsilon = 27200$ and 11700 M^{-1} cm^{-1} for the organosilane

(23) Hori, H.; Koike, K.; Ishizuka, M.; Takeuchi, K.; Ibusuki, T.; Ishitani, O. *J. Organomet. Chem.* **1997**, *530*, 169–176.
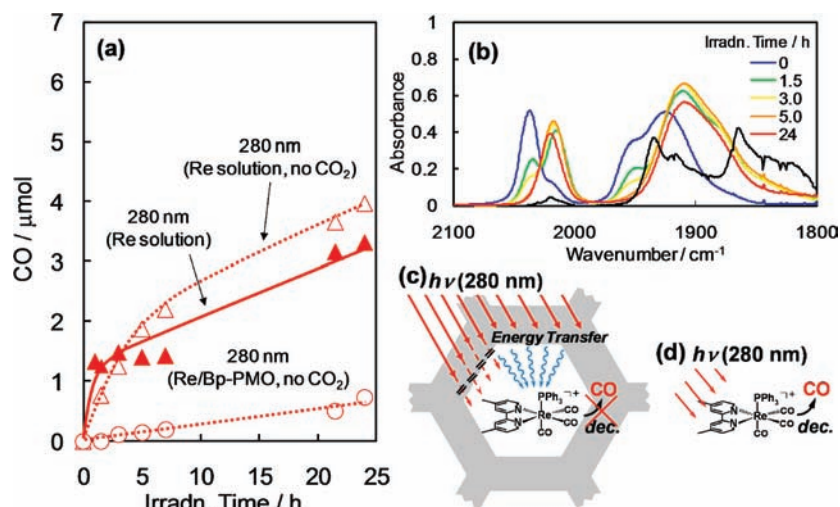
Figure 6. Suppression of CO ligand dissociation from $[Re(BPy)(CO)_3(PPh_3)]^+$ in Bp-PMO. (a) CO generation from a $[Re(dmb)(CO)_3(PPh_3)]^+$ homogeneous solution (0.06 mM; Re: 3 μmol) under photoirradiation at 280 nm with (▲) and without (△) CO_2 in the atmosphere. CO generation from Re/Bp-PMO (Re: 3 μmol) under photoirradiation at 280 nm without CO_2 in the atmosphere (○). (b) FT-IR spectral changes in the CO stretching region of Re/Bp-PMO during photocatalytic CO_2 reduction for 0−24 h. FT-IR spectra of a $[Re(dmb)(CO)_3(PPh_3)]^+$ homogeneous solution after photoirradiation at 280 nm for 24 h under an Ar atmosphere (black). (c) Schematic representations of the protection effect of Bp-PMO from (d) the CO-ligand dissociation of $[Re(dmb)(CO)_3(PPh_3)]^+$ by UV irradiation.

precursor (1,4-bis(triethoxysilyl)biphenyl; BTEBP) and *fac*-$[Re(dmb)(CO)_3(PPh_3)]^+$, respectively, at 260 nm) and the molar ratio of Re/Bp (0.11). The measurement of the excited state lifetime of Re/Bp-PMO also indicated dynamic quenching of the Bp excited state in the presence of the Re complex (Supporting Information, Figure S2). Thus, the light-energy captured on the Bp-PMO antenna was efficiently funneled into the Re complex mainly by the RET mechanism.

The photocatalysis of CO_2 reduction was evaluated for Re/Bp-PMO (10 mg) dispersed in a mixture of an organic solvent (CH_3CN) and a sacrificial agent (triethanolamine; TEOA) (5:1 v/v, 50 mL). Monochromic light irradiation at 280 nm (excitation of Bp) under a CO_2 atmosphere generated CO (Figure 5). For initial 5 h, CO was constantly evolved with an apparent quantum yield (Φ_{CO}^{app}) of 1.2%, as estimated from the linear CO evolution rate and the light intensity (1.7 × 10^{-8} einstein s^{-1}). The total CO production for 24 h reached 6.2 μmol, which corresponds to a turnover number (TN_{CO}) of 2.2 based on the amount of Re atoms (2.9 μmol) in the slurry, although the catalyst was gradually deactivated after 5 h. The $^{13}CO_2$ (>99 atom % enriched) tracer experiment produced 5.6 μmol of CO (over 24 h) consisting of ^{13}CO (68%) and ^{12}CO (32%) (Supporting Information, Figure S3). The presence of ^{12}CO can be reasonably explained by a ligand exchange from ^{12}CO to ^{13}CO in the photocatalytic cycle,[17] which was also confirmed by FT-IR spectroscopy of the recovered sample (Supporting Information, Figure S3c). On the other hand, the tricarbonyl structure ($[Re(BPy)-(CO)_3L]^+$, L = PPh_3 or $OCHO^-$) was completely preserved for Re/Bp-PMO without CO dissociation during the photoreaction, as discussed later. No CO was detected for Bp-PMO without the Re complex under photoirradiation at 280 nm, which indicates that the evolved CO does not originate from the organic component (Bp) of Bp-PMO (Figure 5). These results clearly show the photocatalytic formation of CO from CO_2 by Re/Bp-PMO.

Photoirradiation to Re/Bp-PMO at 365 nm (direct excitation of the Re complex) with the same light intensity (1.7 × 10^{-8} einstein s^{-1}) resulted in a smaller amount of CO

evolution (1.4 μmol for 24 h) (Figure 5). A homogeneous solution of *fac*-$[Re(dmb)(CO)_3(PPh_3)]^+$ also evolved a small amount of CO (1.4 μmol for 24 h at 365 nm) in CH_3CN/TEOA (5:1 v/v, 50 mL) with the same amount of the Re complex (3 μmol, 0.06 mM) in the reaction vessel as that in Re/Bp-PMO (Figure 5).[24] Comparison of the amounts of CO evolved from Re/Bp-PMO under irradiation at 280 and 365 nm for 24 h indicates that the excitation of Bp enhanced the photocatalysis of the Re complex by a factor of 4.4 (Figure 1). This result clearly shows an antenna effect of Bp-PMO for enhancing the photocatalysis of the Re complex. However, the antenna effect should be much larger than the observed value because the absorption efficiency of the Bp groups is approximately 99 times larger than that of the Re complex in Re/Bp-PMO, as estimated from the Bp/Re ratio (9.1) and the molar extinction coefficients of BTEBP ($\varepsilon = 15200$ M^{-1} cm^{-1} at 280 nm) and *fac*-$[Re(dmb)(CO)_3(PPh_3)]^+$ ($\varepsilon = 1400$ M^{-1} cm^{-1} at 365 nm) in CH_3CN. The deviation was mainly attributed to a smaller difference in the actual absorption efficiency under irradiation at 280 and 365 nm for the Re/Bp-PMO suspension because of a smaller penetration length of 280 nm light than that of 365 nm light.

The Bp-PMO antenna showed an additional advantage in stabilization of the Re complex in the mesochannels against UV light. Irradiation of a homogeneous solution of *fac*-$[Re-(dmb)(CO)_3(PPh_3)]^+$ at 280 nm evolved a considerable amount of CO gas (132 mol % CO/Re complex after 24-h irradiation), regardless of the presence of CO_2 (Figure 6a), because of CO ligand dissociation from Re complexes, which has been known to result from the formation of vibrationally hot states of the Re complexes by absorption of high-energy UV light ($\lambda < 313$ nm).[25] However, Re/Bp-PMO showed a much smaller amount of CO generation (8.3%) than that for the homogeneous Re complex solution under

(24) Hori, H.; Johnson, F. P. A.; Koike, K.; Takeuchi, K.; Ibusuki, T.; Ishitani, O. *J. Chem. Soc., Dalton Trans.* **1997**, 1019–1023.
(25) Sato, S.; Sekine, A.; Ohashi, Y.; Ishitani, O.; Blanco-Rodríguez, A. M.; Vlček, A., Jr.; Unno, T.; Koike, K. *Inorg. Chem.* **2007**, *46*, 3531–3540.

irradiation at 280 nm without CO_2 in the atmosphere (Figure 6a). The FT-IR spectra of the recovered Re complexes after 24 h UV-light irradiation revealed the formation of Re biscarbonyl complexes (1936 and 1866 cm^{-1}) such as $[Re(dmb)(CO)_2(PPh_3)_2]^+$ (m/z = 951.2 from ESI-MS; Supporting Information, Figure S4) and Re monocarbonyl complexes (1825 cm^{-1}) for the naked Re complex (in solution), but not for Re/Bp-PMO (Figure 6b, black). Suppression of the CO ligand dissociation for Re/Bp-PMO can be explained by the lack of a formation of higher excited states of Re such as, $^1\pi-\pi^*$ because of absorption of high-energy photons by the Bp-PMO antenna, followed by relaxation to the lowest excited or excimer states of Bp and transfer to the Re complex making its ^{1}MLCT and ^{3}MLCT by first intersystem crossing (Figure 6c). The FT-IR spectra also showed that the Re complex in Bp-PMO gradually changed to Re-formato species $[Re(BPy)(CO)_3(OCHO)]$ (2018, 1912, and 1894 cm^{-1}) with almost complete formation during the photoreaction taking 5 h (Figure 6b). A formation of the Re-formato complex by ligand substitution from PPh$_3$ to OCHO$^-$ is also well-known as a deactivation process in a homogeneous fac-$[Re(dmb)(CO)_3(PPh_3)]^+$ system during photocatalytic CO_2 reduction.[24] The formation of the formato complex would cause the deactivation of Re/Bp-PMO for photocatalysis of CO_2 reduction (Figure 5). However, the time-course of the deactivation for Re/Bp-PMO is much longer than that for homogeneous fac-$[Re(dmb)(CO)_3-(PPh_3)]^+$ which usually forms the Re-formato complex within a few tens of minutes.[24] Fixation of the Re complex in the mesochannels would hinder a chain reaction between one-electron reduced and original Re complexes,[24] which would suppress dissociation of the PPh$_3$ ligand from the Re complex and the subsequent formation of the deactivated Re-formato species.

Conclusion

Co-condensation of two organosilane precursors containing bridged biphenyl group and terminal bipyridine ligand in the presence of a template surfactant afforded BPy-Bp-PMO in which the bipyridine ligand was anchored on the walls of the mesochannels of Bp-PMO. The subsequent coordination of the Re precursor to the bipyridine unit gave Re/Bp-PMO in which the Re complexes are homogeneously fixed on the walls of the mesochannels. The light energy absorbed effectively by the biphenyl groups in Bp-PMO was funneled into the Re complex by RET and sensitized photocatalytic CO evolution from CO_2 by a factor of 4.4 compared with direct excitation of the Re complex because of the light-harvesting of the PMO antenna. The PMO antenna also showed a photoprotection effect on CO-ligand dissociation from the Re complex by UV-light irradiation. These results evidently demonstrate the potential of PMOs as a light-harvesting antenna for designing various photocatalytic systems using PMOs[9c,26] mimicking the natural photosynthesis.

Supporting Information Available: Complete ref 2a, detailed description of CO quantification, excitation lifetime of the Re/Bp-PMO, GC-MS analysis of the evolved gas and FT-IR spectrum of the rhenium complex after photocatalysis of Re/Bp-PMO under a $^{13}CO_2$ atmosphere, and ESI-MS analysis of the rhenium complex after photzodecomposition of $[Re(dmb)(CO)_3-(PPh_3)](PF_6)$. This material is available free of charge via the Internet at http://pubs.acs.org.

(26) (a) Maegawa, Y.; Goto, Y.; Inagaki, S.; Shimada, T. *Tetrahedron Lett.* **2006**, *47*, 6957–6960. (b) Goto, Y.; Nakajima, K.; Mizoshita, N.; Suda, M.; Tanaka, N.; Hasegawa, T.; Shimada, T.; Tani, T.; Inagaki, S. *Microporous Mesoporous Mater.* **2008**, *117*, 535–540. (c) Takeda, H.; Goto, Y.; Maegawa, Y.; Ohsuna, T.; Tani, T.; Matsumoto, K.; Shimada, T.; Inagaki, S. *Chem. Commun.* **2009**, 6032–6034.